

# Material Properties of the Post-Mortem Small Intestine in High-Rate Equibiaxial Elongation

Meghan K. Howes and Warren N. Hardy  
Virginia Tech-Wake Forest University, Center for Injury Biomechanics

## ABSTRACT

*Motor vehicle collisions (MVCs) are the most common cause of small intestine injuries and the accompanying mesenteric injuries that occur due to blunt trauma. Crash-induced injuries of the intestine include lacerations, serosal tears, and perforations. To characterize the biomechanical response of the small intestine associated with these injury modes, the multidirectional failure properties of cruciate tissue samples were investigated with high-rate equibiaxial stretch. Tissue testing was conducted on intestine samples harvested from four post-mortem human surrogates. Cruciate samples were stamped from the tissue with the material and stretching axes aligned with the visible longitudinal fiber direction or offset by 22 degrees. Sample arms were gripped in four low-mass tissue clamps and simultaneous motion of four carriages applied equibiaxial stretch in orthogonal directions. Tests were conducted at a target strain rate of  $100\text{s}^{-1}$  to investigate tissue failure properties at rates expected to be experienced in MVCs. Load and acceleration were measured at each carriage. Laser displacement sensors were used to obtain changing sample thickness. All data were captured using 20ksps. True stress and 2<sup>nd</sup> Piola Kirchhoff stress were computed and transformed to align with the material axes. Overhead high-speed video captured at 2500fps provided optical marker displacement data. Marker positions were tracked using motion analysis software. Displacement data were input into LS-DYNA, and average Green-Lagrange strain was calculated at 0.05-ms intervals. All data were truncated at tear initiation determined from high-speed video analysis. Results from 28 small intestine tests indicated an average maximum principal strain rate of  $86.7 \pm 25.9\text{s}^{-1}$  and an average maximum principal failure strain of  $0.270 \pm 0.083$ . Average Green-Lagrange failure strain was  $0.169 \pm 0.060$  in the circumferential direction and  $0.169 \pm 0.068$  in the longitudinal direction. Average peak 2<sup>nd</sup> Piola Kirchhoff stress ranged from 3 to 5MPa with a trend toward a stiffer response in the longitudinal direction. Tests conducted in this study identify failure thresholds for the small intestine loaded in equibiaxial stretch at rates expected to be experienced in MVCs.*

## INTRODUCTION

Risk of serious abdominal injury in motor vehicle collisions (MVCs) is substantially reduced with the proper use of seatbelts (Klinich et al., 2010). However, a significant increase in the occurrence of gastrointestinal tract injury exists with belt loading (Rutledge et al., 1991). Crash-induced injuries of the small intestine occurring in MVCs include lacerations, serosal

tears, perforations, and accessory mesenteric injuries (Appleby and Nagy, 1989; Munns et al., 1995). To characterize the biomechanical response of the small intestine associated with these injuries, stress and strain data from high-rate, multidirectional testing to failure must be analyzed.

Uniaxial tissue testing is often conducted as an initial attempt to characterize the tensile response of soft tissues. Samples are typically unconstrained in the transverse direction; therefore, uniaxial testing provides a high strain, low stress mechanical environment. Biaxial material testing provides a high stress, low strain mechanical environment (Lanir and Fung, 1974; Demer and Yin, 1983) and is conducted to more accurately match multi-axial loading and failure modes experienced *in vivo*. In general, little biomechanical data exist specific to the hollow abdominal organs. Further, existing material property data for the human post-mortem small intestine is limited to the uniaxial, quasi-static tensile response (Egorov et al., 2002). Biaxial testing was conducted in this study to define the failure properties of the post-mortem small intestine at rates expected to be experienced in MVCs.

## METHODS

### Sample Preparation

Tissue testing was conducted on samples harvested from four post-mortem human surrogates (PMHS). All surrogates were male with average age of 76 years, average stature of 179cm, and average mass of 93kg. The excised intestine of each surrogate was divided into rectangular tissue sections devoid of visible inhomogeneities that might affect the response of the tissue samples. Tissue sections were opened along the mesenteric border, and cruciate-shaped samples were obtained using a custom stamp applied with an arbor press. The cruciate stamp was aligned with the visible longitudinal fiber direction or offset from the fiber direction by 22 degrees. The offset minimizes error in material parameter determination (Lanir et al., 1996) and prevents failure across the arm branches of the sample (Shah et al., 2006). This resulted in failure through the ROI such that the local strain calculated in the ROI was a direct measure of the failure strain. Procurement to testing time was minimized for all tissues. Between procurement and testing, samples were stored in saline-soaked gauze in airtight containers at 34°F. Normal saline spray was used to maintain sample hydration during positioning in the test apparatus. Samples were positioned in the tester with the mucosa in view of an overhead high-speed video camera. Optical markers were applied to the sample surface using indelible ink. All testing was conducted at ambient temperature.

### Test Configuration

Biaxial testing was conducted using a custom test apparatus designed to apply large, multidirectional strain at high rates. A detailed description of the device is presented by Mason et al. (2005). Sample arms were gripped in four low-mass tissue clamps and simultaneous motion of four carriages applied equibiaxial stretch in four orthogonal directions (Figure 1). Tests were conducted at a target strain rate of  $100\text{s}^{-1}$  to investigate failure at rates expected to be experienced

in MVCs. Samples were stretched until complete transection occurred. Miniature load cells (ELFF-T2E-100lb, Measurement Specialties, CA) were used to measure applied load at each tissue clamp. Miniature accelerometers (3038-500g, Measurement Specialties, CA) were mounted to each carriage for inertial compensation of the measured load. Laser displacement sensors (LK-G157, Keyence Corporation, NJ) mounted above and below the sample were used to obtain changing sample thickness in a central region of interest (ROI) of the sample throughout the test duration. Sample thickness was calculated using a calibrated difference in recorded measurement from the upper and lower sensors. All data were captured using 20ksps. Overhead high-speed video (Phantom v9.1, Vision Research, NJ) captured at 2500fps provided optical marker displacement data in the ROI of the sample at a resolution of 7px/mm.

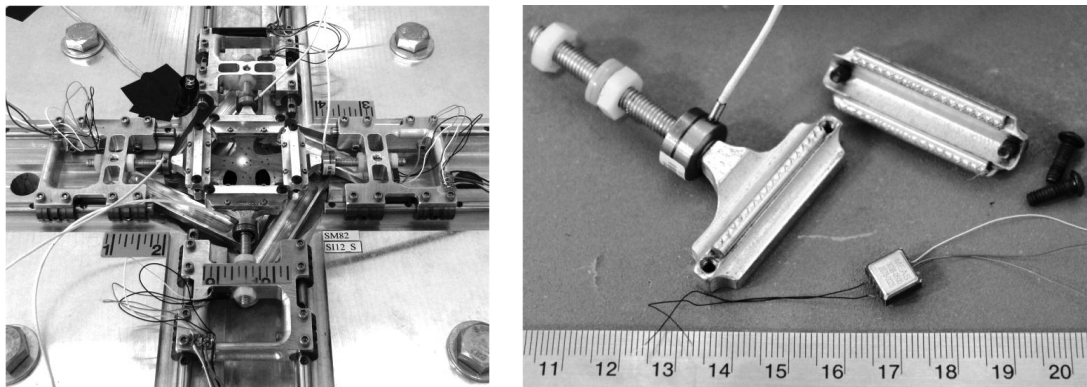


**Figure 1:** Dynamic biaxial test apparatus and tissue clamp components.

## Data Processing and Analysis

All data were zeroed at the time corresponding to the initiation of carriage movement determined from high-speed video analysis. Failure was defined as tear initiation determined from the high-speed video. All data were truncated at the time of tear initiation as the purpose of this work was to obtain response and tolerance to failure, and the subsequent tear propagation requires a more complex analysis. Multidirectional displacement data were obtained by tracking the position of five markers in the ROI using motion analysis software (TEMA, Image Systems, Linköping, Sweden) employing a regional correlation method (Figure 2). Displacement data for each marker were input into LS-DYNA as boundary prescribed motion for five nodes. Marker triads sectioned the ROI into four triangular shell elements. Green-Lagrange strain, maximum principal strain, and maximum shear strain were determined as the average value from each of the four elements solved at 0.05ms time intervals. Green-Lagrange strain for each element corresponds to the strain tensor (Eqn. 2) calculated from the deformation gradient computed for each marker triad (Eqn. 1). The stretch ratio ( $\lambda$ ) and true strain ( $\epsilon$ ) were calculated from the Green-Lagrange strain (Eqn. 3). Maximum principal strain corresponds to the eigenvalues ( $\lambda_{\pm}$ ) of the Green-Lagrange strain tensor (Eqn. 4). Average maximum principal strain rate was calculated as the average of the time derivative of the maximum principal strain over the test duration. All data were transformed to align with the material axes of the tissue.

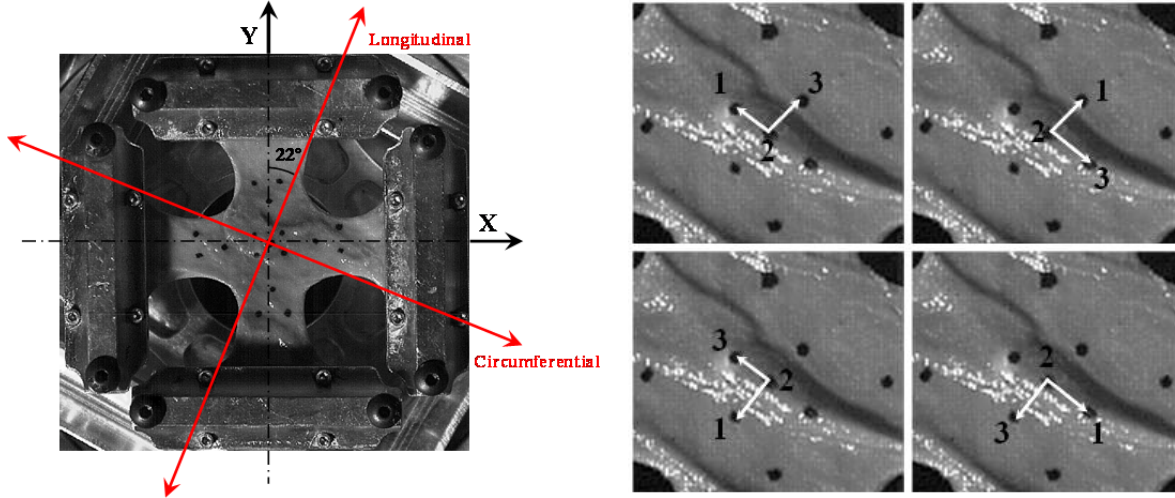


**Figure 2:** Sample alignment and optical marker triads.

$$\mathbf{F} = \left( \begin{bmatrix} X_1 & X_2 \\ Y_1 & Y_2 \end{bmatrix}_{t=1} \right) \left( \begin{bmatrix} X_1 & X_2 \\ Y_1 & Y_2 \end{bmatrix}_{t=0} \right)^{-1} \quad \text{Eqn. 1}$$

$$\mathbf{E} = \begin{bmatrix} E_{11} & E_{12} \\ E_{21} & E_{22} \end{bmatrix} = \frac{1}{2} (\mathbf{F}^T \mathbf{F} - \mathbf{I}) \quad \text{Eqn. 2}$$

$$\varepsilon = \ln \lambda = \ln \sqrt{2E + 1} \quad \text{Eqn. 3}$$

$$\lambda_{\pm} = \frac{1}{2} \left[ (E_{11} + E_{22}) \pm \sqrt{4E_{12}E_{21} + (E_{11} - E_{22})^2} \right] \quad \text{Eqn. 4}$$

Effective mass used for inertial compensation of each measured load was optimized for each of the four clamps for each tissue test. Compensated load for each clamp was adjusted to the ROI by applying an assumption of a proportional transmission of load through each arm to the central region. A scaling ratio of the initial length of the ROI obtained from the outer marker pairs to the initial sample arm width in the same direction was applied to scale the normal load at each time step. Two compensated loads measured in each direction were averaged to obtain the load-time history in the x- and y-directions. True stress (S) was calculated using the changing cross-sectional area determined from the laser thickness data filtered at SAE J211 Channel Frequency Class (CFC) 180 and the changing ROI length (Eqn. 5). 2<sup>nd</sup> Piola Kirchhoff stress (K) was calculated from the initial cross-sectional area and the inverse of the stretch ratio (Eqn. 6). Stress data were filtered at CFC 600. For samples with the material and stretching axes offset, the data were transformed to align with the material axes. Only 2<sup>nd</sup> Piola Kirchhoff stress will be included in the results of this analysis.

$$S = \frac{P}{A_{n\perp}} \quad \text{Eqn. 5}$$

$$K = \frac{P}{A_{0\perp}} * \frac{1}{\lambda_{\parallel}} \quad \text{Eqn. 6}$$

## RESULTS

A total of 28 high-rate equibiaxial tension tests were conducted on small intestine samples harvested from four PMHS (Figure 3). Directional Green-Lagrange strain, maximum principal strain, and maximum shear strain were computed (Figure 4). Averages and standard deviations were truncated at the shortest test duration. Average strain rate was  $86.7 \pm 25.9 \text{ s}^{-1}$ . Average maximum principal strain at failure was  $0.270 \pm 0.083$ . Average failure strain was  $0.169 \pm 0.060$  in the circumferential direction and  $0.169 \pm 0.068$  in the longitudinal direction. Failure strain is shown in Figure 5. Two-sample Student's t-tests assuming unequal variances were used to assess significance in failure strain by direction ( $\alpha=0.05$ ). The difference in failure strain in the circumferential and longitudinal directions was not statistically significant ( $p=0.99$ ).

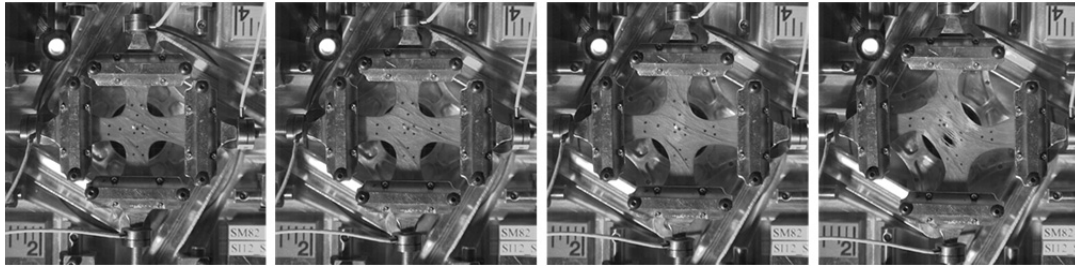


**Figure 3:** High-speed video stills from a typical offset small intestine test.

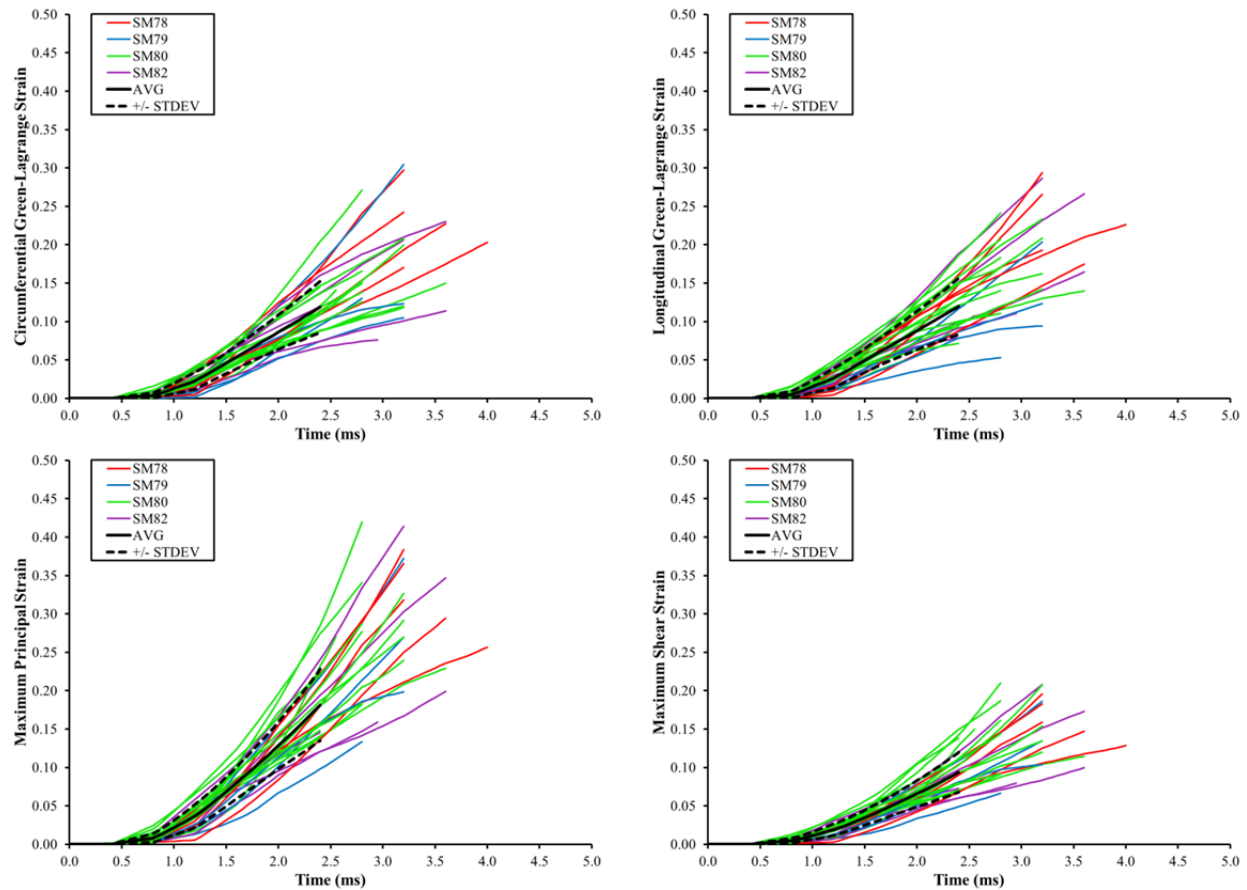


**Figure 4:** Directional Green-Lagrange strain, maximum principal strain, and maximum shear strain.

Peak directional 2<sup>nd</sup> Piola Kirchhoff stress was determined for each test (Figure 5). Average peak stress was  $2.82 \pm 2.46$  MPa in the circumferential direction and  $4.42 \pm 3.15$  MPa in the longitudinal direction. For all samples, the peak stress in the longitudinal direction was greater than in the circumferential direction. Student's t-tests assuming unequal variances were used to assess significance in peak stress by direction ( $\alpha=0.05$ ). The difference in peak stress was statistically significant for the circumferential and longitudinal directions ( $p=0.04$ ).

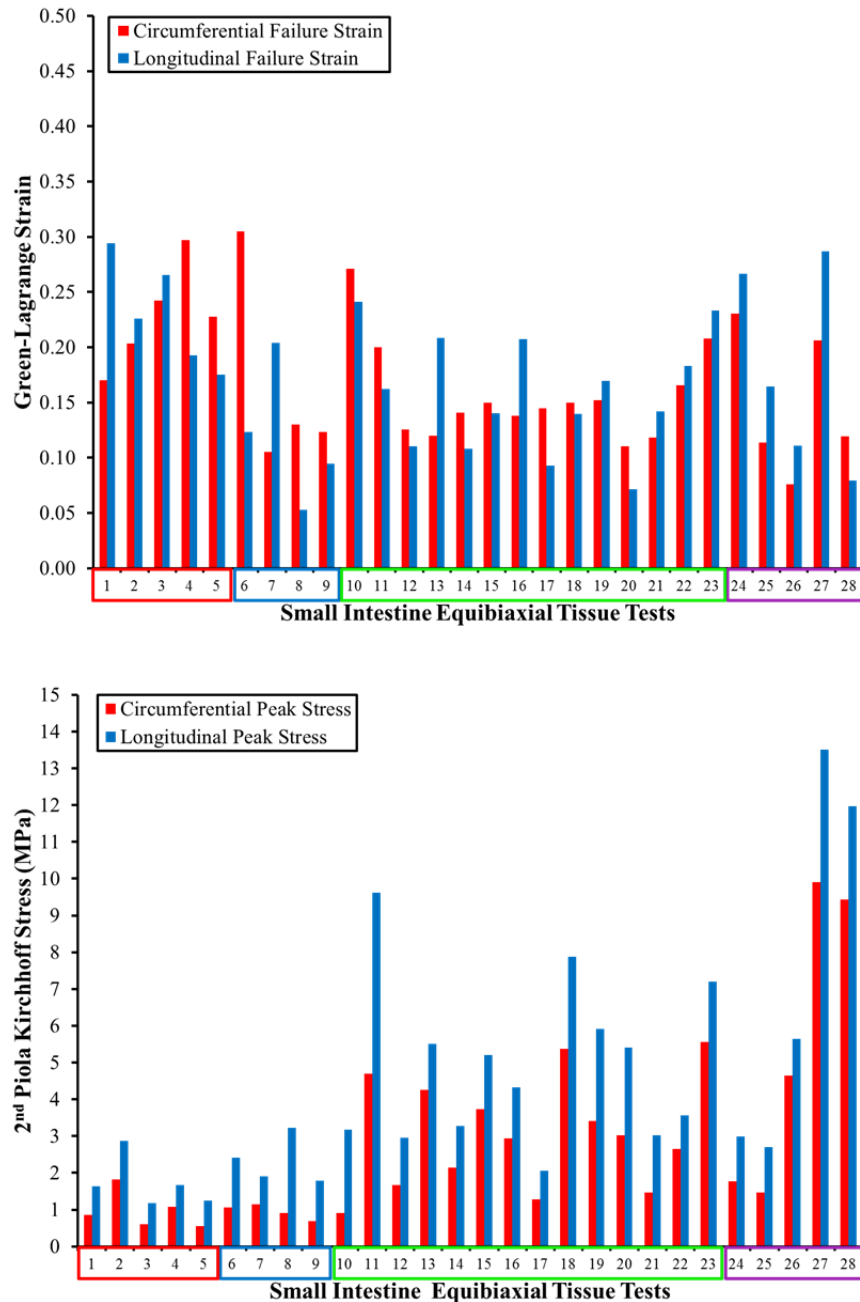


**Figure 5:** Directional failure strain and peak stress with axes indicating samples from each PMHS.

## DISCUSSION

Multidirectional stress and strain results were presented for 28 biaxial small intestine tests conducted at dynamic rates. Failure strain was calculated as an average failure strain for the central ROI. Directional failure strain was not statistically significant for these tests. The difference in directional peak stress in the ROI was statistically significant with a greater peak stress occurring in the longitudinal direction for each test. A stiffer response in the longitudinal direction may be attributed to a lower resistance to stretch in the circumferential direction related to the physiologic need for expansion of the bowel during digestion.

Shear strain was minimized for these tests. Uneven sample geometry, slip between sample layers, and rotation or vibration of the sample arms increases the shear strain. Shear strain was minimized by maintaining short and equal sample arm length and ensuring even sample geometry for all four arms. A target maximum shear strain of less than ten percent prior to tissue failure was considered reasonable, indicating that multi-axial stretch was achieved with minimal shear in the ROI. The compliant nature of small intestine tissue resulted in exceeding ten percent maximum shear strain only immediately prior to tear initiation for these tests.

Results of the biaxial testing are only applicable *in vitro* and do not directly describe the *in vivo* response of the tissue. Efforts were made to maintain repeatable initial test conditions for all samples; however, these conditions may not match the physiologic stress or strain state experienced *in vivo*. Further, the measured response of the small tissue samples may not be representative of the whole organ response (Sacks, 2000). Despite these limitations, it is important to acquire component-level material property data for the development and validation of finite element model components.

## CONCLUSIONS

A methodology for high-rate equibiaxial tissue testing was presented along with the stress and strain results of 28 small intestine tests. Samples were harvested from four PMHS and tested at a dynamic maximum principal strain rate of  $86.7 \pm 25.9 \text{ s}^{-1}$ . Average Green-Lagrange failure strain was  $0.169 \pm 0.060$  and  $0.169 \pm 0.068$  in the circumferential and longitudinal directions, respectively. Average 2<sup>nd</sup> Piola Kirchhoff peak stress was  $2.82 \pm 2.46 \text{ MPa}$  in the circumferential direction and  $4.42 \pm 3.15 \text{ MPa}$  in the longitudinal direction. Material property data acquired in this study contribute to the biomechanical characterization of the abdominal organs in high-rate multi-axial elongation.

## ACKNOWLEDGMENTS

A portion of this work was funded by the Global Human Body Models Consortium, LLC.

## REFERENCES

- APPLEBY, J.P. and NAGY, A.G. (1989). "Abdominal Injuries Associated with the Use of Seatbelts," *Am J Surg*, vol. 157, pp. 457-458.
- DEMER, L.L. and YIN, F.C. (1983). "Passive Biaxial Mechanical Properties of Isolated Canine Myocardium," *J Physiol*, vol. 339, pp. 615-630.
- EGOROV, V.I., SCHASTLIVTSEV, I.V., PRUT, E.V., BARANOV, A.O., TURUSOV, R.A. (2002). "Mechanical Properties of the Human Gastrointestinal Tract," *J Biomech*, vol. 35, pp. 1417-1425.
- KLINICH, K.D., FLANNAGAN, C.A.C., NICHOLSON, K., SCHNEIDER, L.W., RUPP, J.D. (2010). "Factors Associated with Abdominal Injury in Frontal, Farside, and Nearside Crashes," *Stapp Car Crash J*, vol. 54, pp. 73-91.
- LANIR, Y. and FUNG, Y.C. (1974). "Two-Dimensional Mechanical Properties of Rabbit Skin. II. Experimental Results," *J Biomech*, vol. 7, pp. 171-182.
- LANIR, Y., LICHTENSTEIN, O., IMANUEL, O. (1996). "Optimal Design of Biaxial Tests for Structural Material Characterization of Flat Tissues," *J Biomech Eng*, vol. 118, pp. 41-47.
- MASON, M.J., SHAH, C.S., MADDALI, M., YANG, K.H., HARDY, W.N., VAN EE, C.A., DIGGES, K. (2005). "A New Device for High-Speed Biaxial Tissue Testing: Application to Traumatic Rupture of the Aorta," SAE Paper No. 2005-01-0741.
- MUNNS, J., RICHARDSON, M., HEWETT, P. (1995). "A Review of Intestinal Injury from Blunt Abdominal Trauma," *Aust NZ J Surg*, vol. 65, pp. 857-860.
- RUTLEDGE, R., THOMASON, M., OLLER, D., MEREDITH, W., MOYLAN, J., CLANCY, T., CUNNINGHAM, P., BAKER, C. (1991). "The Spectrum of Abdominal Injuries Associated with the Use of Seat Belts," *J Trauma*, vol. 31, pp. 820-825.
- SACKS, M.S. (2000). "Biaxial Mechanical Evaluation of Planar Biological Materials," *Journal of Elasticity*, vol. 61, pp. 199-246.
- SHAH, C.S., HARDY, W.N., MASON, M.J., YANG, K.H., VAN EE, C.A., MORGAN, R., DIGGES, K. (2006). "Dynamic Biaxial Tissue Properties of the Human Cadaver Aorta," *Stapp Car Crash J*, vol. 50, pp. 217-246.